p85β phosphoinositide 3-kinase subunit regulates tumor progression

Isabel Cortés[a], Jesús Sánchez-Ruíz[a], Susana Zuluaga[a], Vincenzo Calvanese[a], Miriam Marqués[b], Carmen Hernández[a], Teresa Rivera[c], Leonor Kremer[d], Ana González-García[a], and Ana C. Carrera[a,1]

[a]Department of Immunology and Oncology and [d]Protein Tools Unit, Centro Nacional de Biotecnología/Consejo Superior de Investigaciones Científicas, Universidad Autónoma de Madrid, 28049 Madrid, Spain; [b]Epithelial Carcinogenesis, Department of Molecular Pathology, Spanish National Cancer Research, 28029 Madrid, Spain; and [c]Human Pathology Service, Hospital Universitario de Móstoles, 28935 Madrid, Spain

Edited by Jonathan M. Backer, Albert Einstein College of Medicine, Bronx, NY, and accepted by the Editorial Board May 29, 2012 (received for review November 4, 2011)

PIK3R2 **encodes a ubiquitous regulatory subunit (p85β) of PI3K, an enzyme that generates 3-polyphosphoinositides at the plasma membrane. PI3K activation triggers cell survival and migration. We found that p85β expression is elevated in breast and colon carcinomas and that its increased expression correlates with PI3K pathway activation and tumor progression. p85β expression induced moderate PIP_3 generation at the cell membrane and enhanced cell invasion. In accordance, genetic alteration of *pik3r2* expression levels modulated tumor progression in vivo. Increased p85β expression thus represents a cellular strategy in cancer progression.**

Activation of class I PI3K is involved in the pathogenesis of cancer. PI3Ks are lipid kinases that phosphorylate membrane phosphoinositides [i.e., phosphatidylinositol (PtdIns)] to generate PtdIns(3,4)P_2 (PIP_2) and PtdIns(3,4,5)P_3 (PIP_3). PI3K is composed of a regulatory and a p110 catalytic subunit. Four genes encode the highly conserved p110 catalytic subunit (*PIK3CA*, *CB*, *CD*, and *CG*). p110α, β, and δ associate with p85 regulatory subunits and are activated mainly by growth factor receptors; p110γ associates with distinct regulatory subunits and is activated preferentially by G protein-coupled receptors (1–3). Three genes encode p85-type regulatory subunits: *PIK3R1* (p85α, p55α, p50α), *PIK3R2* (p85β), and *PIK3R3* (p55γ). *R1* and *R2* are ubiquitously expressed and *R3* expression is tissue-restricted (4).

p85β is expressed at lower levels than p85α in most tissues (5–7). Whereas mice deficient in *Pik3r2* develop normally and exhibit only moderate metabolic and immunological defects (7) *Pik3r1*$^{-/-}$ mice die perinatally (8). p85α controls p110 stability and blocks p110 activity during quiescence (9). The inhibitory role of p85α on p110 activity explains why WT *PIK3R1* expression is normally reduced in tumors, and that p85α mutations that relieve p110 from p85 inhibition have been found in cancer (10). Despite extensive analysis of p85α mutations in tumors (10–12), p85β involvement in cancer is less well studied. Here we analyzed the potential contribution of p85β in cancer.

Results

p85β Expression Is Increased in Breast and Colon Carcinomas. By using microarray technology, we performed a preliminary survey of the expression of the genes that form part of the PI3K pathway in a collection of clinical breast (n = 14) and colon carcinomas (n = 12). Comparison of PI3K subunit expression showed that mRNA levels of *PIK3R2* (which encodes p85β) were increased in nearly half the carcinoma samples examined, whereas *PIK3R1* (which encodes p85α) was decreased (Fig. S1). To study this finding in more detail, we compared 20 colon adenocarcinomas (CCs) and 35 breast carcinomas (BCs) with normal surrounding tissue. Tumor and normal samples had comparable numbers of epithelial cells, and normal tissue had a low percentage of malignant cells (0–10%).

To evaluate p85β expression levels, we prepared extracts from normal and tumor samples and analyzed p85 levels by Western blot (WB). We generated anti-p85β Abs and used the 1C8 Ab for further analysis (Fig. S2). For each sample, we measured p85β and p85α band intensity in the linear range, and normalized these to the actin content (Fig. 1*A*). Each sample was analyzed three times, and mean values were used for sample classification based on p85β expression. We confirmed the ranking of p85β and p85α expression by examination of tumor samples in parallel with internal control extracts of HeLa, U2OS, and Jurkat cells; this last cell type expressed similar p85β and p85α levels (7) (Fig. 1*B*). In most normal tissues, p85α is expressed at higher levels than p85β (5–7). In contrast, many CC (55%) and BC (45%) samples showed increased p85β expression and a decrease in p85α (Figs. 1 and 2).

Increased p85β Levels Correlate with Tumor Progression. To determine whether an increase in p85β expression affects PI3K pathway activation, we analyzed phosphorylation of the PI3K effector protein kinase B [PKB; i.e., phosphorylated PKB (pPKB)] by WB. We measured pPKB signal intensity, normalized it for PKB levels (i.e., pPKB/PKB), and calculated the pPKB/PKB ratio in tumor vs. normal tissue (Fig. 1*C*); protein loading was controlled relative to actin. We confirmed PI3K pathway activation by immunohistochemistry (IH) analysis of S6 phosphorylation. S6 kinase activation is generally downstream of PI3K (13) and yielded a better IH signal than pPKB (Fig. 1*D*). Increased pPKB (by WB) and phosphorylated pS6 (pS6; by IH) were correlated in most samples (93%; Fig. 1*D* and Figs. S3 and S4); in the very few samples with normal pPKB and increased pS6, p70S6K could be activated in a PI3K/PKB-independent manner (13). We sequenced *PIK3CA* (mutated in BC) and *K-Ras* (mutated in CC) in the 20 CC and 20 BC samples. *PTEN* mRNA levels (i.e., loss of heterozygosity in BC) (12) were determined by quantitative PCR (qPCR) and confirmed in WB (Figs. S3–S7*A*).

The PI3K pathway was activated in ∼30% of BC and ∼50% of CC samples (Fig. 2*A* and Figs. S3 and S4). Moreover, p85β levels correlated with PI3K pathway (i.e., pPKB/PKB) activation and tumor progression in BC and CC (Fig. 2*A*). We have used Dukes staging to define CC progression, as it describes CC penetration into deep colon layers and other organs. In BC, the Bloom–Richardson criteria classify tumors according to cell differentiation; thus, progression was evaluated as the percentage of affected lymph nodes (14, 15). pPKB activation was not exclusively found in samples with *PIK3CA* or *K-Ras* mutations, decreased *PTEN* levels (Figs. S3–S7), or increased *PKB* levels, as determined by qPCR. BC can be classified as luminal, HER2-

Author contributions: A.C.C. designed research; I.C., J.S.-R., S.Z., V.C., M.M., C.H., T.R., A.G.-G., and A.C.C. performed research; L.K. contributed new reagents/analytic tools; T.R., A.G.-G., and A.C.C. analyzed data; and A.C.C. wrote the paper.

The authors declare no conflict of interest.

This article is a PNAS Direct Submission. J.M.B. is a guest editor invited by the Editorial Board.

[1]To whom correspondence should be addressed. E-mail: acarrera@cnb.csic.es.

This article contains supporting information online at www.pnas.org/lookup/suppl/doi:10.1073/pnas.1118138109/-/DCSupplemental.

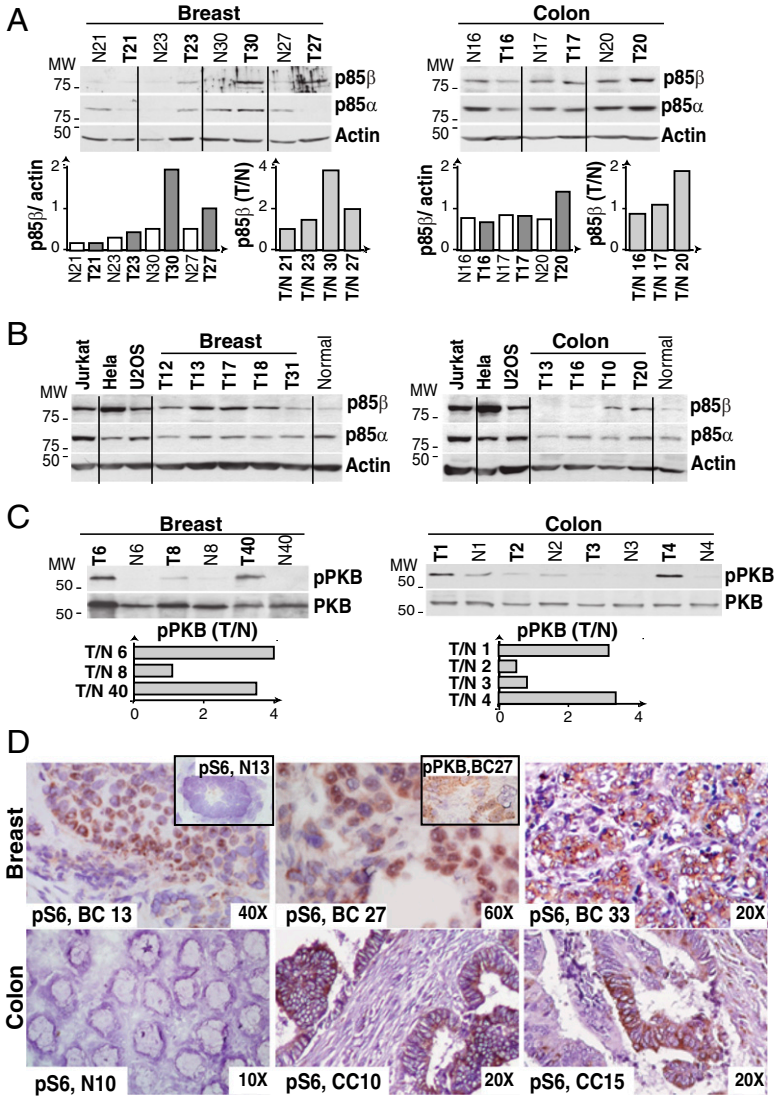

Fig. 1. Increased p85β expression in breast and colon carcinomas. (*A–C*) Extracts from representative CC and BC tumors (T), surrounding normal tissue (N), and control cells (panel *B*) were examined by WB using anti-p85α or anti-p85β Ab (*A* and *B*) or anti-pPKB or anti-PKB Ab (*C*). Graphs show actin-normalized p85β WB signal intensity in each sample, and the increase in p85β levels in T vs. N ratio (*A*) or the ratio of pPKB signal normalized to PKB in T vs. N (C). (*D*) IH of tumor samples using anti-pS6 Ab. BC 13 and 33 show intense staining (score 2.5 of 3) in ~70% of tumor cells; BC 27 shows intermediate staining (score 2) in ~50% of the cells. Inset: Normal acinus and BC27 IH using anti-pPKB Ab. *Lower*: Normal tissue, intense staining in CC10 (score 3, 50% of cells) and intermediate staining in CC15 (score 2, ~45% of cells). Original magnification is indicated.

positive, or basal (16); p85β increase was not selective for any carcinoma subtype (Fig. 2*A*).

To determine whether enhanced p85β levels were a result of increased transcription, we measured *PIK3R2* and *PIK3R1* mRNA levels by triplicate qPCR. *PIK3R1* levels decreased in most tumor samples; in contrast, *PIK3R2* mRNA was often increased in CC and BC (Figs. S5 and S6). It is currently unknown how *PIK3R2* expression is regulated. As *miR126* reduces *PIK3R2* mRNA translation (17), we also measured *miR126* levels, which are regulated by methylation of an upstream CpG island (18). In BC, multiple linear regression analysis showed that p85β levels are a function of increased *PIK3R2* mRNA and reduced *miR126* expression (Fig. 2*B*). CC samples showed the same tendency, although a larger panel is needed to evaluate correlation. Nonetheless, contingency analysis showed that increased p85β levels were more frequent in samples with increased *PIK3R2* as well as in samples with simultaneous increase in *PIK3R2* and reduced *miR126* (Fig. 2*C*).

p85β Enhances Plasma Membrane PIP_3 Levels. To test whether p85β expression increases PI3K activation in normal cells, we expressed p85β/p110α or p85α/p110α at similar levels in immortal murine fibroblasts (NIH 3T3 cells). As PI3K activation increases plasma membrane PIP_3 (1–3), we examined PI3K activation by membrane localization of the GFP-Btk-PH domain, which binds PIP_3 (19). In control quiescent cells, Btk-PH localized to the cytoplasm and nucleus (its size permits nuclear entry), and serum treatment triggered PH localization to the cell membrane (Fig. 3*A*). Even without stimulation, however, p85β/p110α cells (but not p85α/p110α cells) showed PIP_3 at the plasma membrane (Fig. 3*A*) and higher basal PI3K pathway activation (Fig. S7*B*).

To determine whether this action is p110-dependent, we expressed a p85β mutant that does not bind p110 (Δp85β). Δp85β/p110α did not trigger basal membrane PIP_3 localization (Fig. 3*B* and Fig. S7*C*). Transfection of p85β alone also induced slight Btk-PH membrane localization and basal PKB activation; this effect was p110-dependent, as it was not induced by Δp85β and was reduced by PI3K inhibitors (Fig. S7 *D–F*). Overexpression of p85α or p85β alone interfered with serum-induced membrane PIP_3 localization and PKB activation; this interference was lower with p85β (Fig. S7 *D* and *E*). In the absence of stimulus, p85β and p85β/p110α also induced cell elongation, which is normally observed after cell activation (Fig. 3*B* and Fig. S7*E*). This p85β-induced morphological change was p110-independent, as it was also triggered by Δp85β (Fig. 3*B* and Fig. S7 *C* and *E*).

Enhanced PI3K Pathway Activation in p85β-Expressing Cells. We examined PI3K pathway activation in human U2OS cells transfected

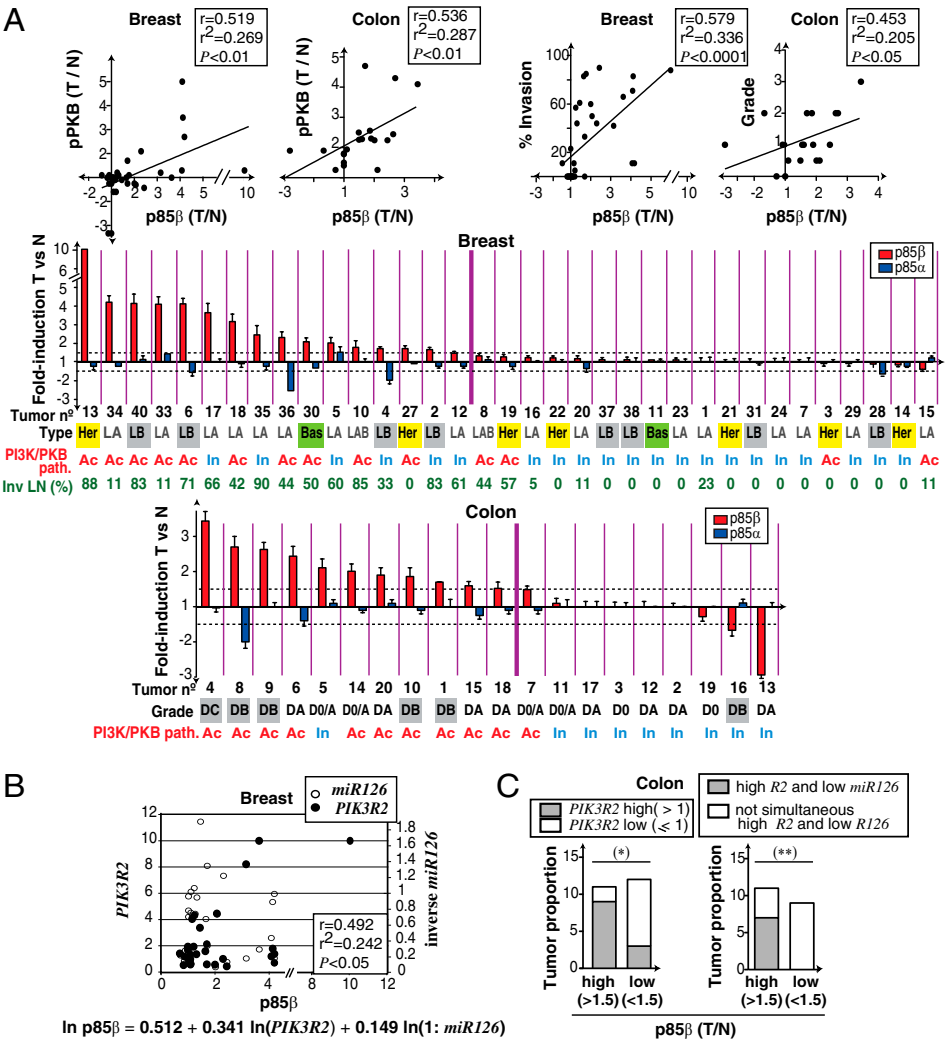

Fig. 2. Increased p85β expression and PI3K pathway activation in advanced tumors. (*A*) Pearson correlation of p85β [tumor (T)/normal (N) ratio] vs. pPKB/PKB (T/N ratio) levels or vs. percentage of invaded LN (breast) or tumor grade (colon). For CC correlation, grade D0 is 0, D0/A is 1.5, DA is 1, DB is 2, and DC is 3. Color graphs show results for p85α and p85β protein expression (T vs. N; mean ± SD, triplicate WB). Horizontal dashed lines indicate a p85β expression change greater or lower than 1.5-fold. Thick vertical line separates tumors with >1.5-fold increase in p85β. Beneath the graphs, tumor number, PI3K/PKB pathway status (Ac, active; In, inactive), CC grade (Dukes grade) or BC type (LA, LB, luminal A or B; LAB, luminal; Her, HER2-positive; Bas, basal), and percentage of invaded lymph nodes (LNs) are indicated. (*B*) Multiple linear regression analysis of p85β (T/N ratio) dependence on *PIK3R2* mRNA and *miR126* levels in BC. We used relative quantity values for *PIK3R2* mRNA and relative quantity values^{-1} for *miR126*. Variables were transformed by the function ln(x + 1). (*C*) CC samples grouped by p85β levels were compared with samples with low or high *PIK3R2* mRNA levels (*Left*) or with simultaneous high *PIK3R2* and low *miR126* levels (≤1; *Right*). *$P < 0.05$ and **$P < 0.01$ by Fisher exact test.

with hemagglutinin (HA)-p85α or HA-p85β and p110α, and confirmed similar expression of p85α and p85β by using anti-HA Ab in WBs (Fig. 4*A*). As in NIH 3T3 cells, unstimulated U2OS cells showed higher pPKB levels in p85β/p110α than in p85α/p110α cells, and p85β alone interfered with serum-induced PKB activation less than p85α (Fig. 4*A*). Finally, in the absence of stimulus in U2OS cells, reduction of p85β levels, but not of p85α levels, reduced PI3K pathway activation (Fig. 4*B*). Cell stimulation is thus necessary for optimal PI3K pathway activation in p85β/p110α- and p85α/p110α-expressing cells. In the absence of stimulus, p85β, but not p85α, triggers basal PI3K pathway activation, as also observed in PTEN$^{-/-}$ cells (20).

p85β/p110α Cells Have Greater Kinase Activity than p85α/p110α for PtdIns(4,5)P_2. The constitutive membrane localization of PIP_3 in p85β/p110α cells could indicate that this complex has a higher intrinsic affinity for membrane phosphoinositides than p85α/p110α. We compared the kinase activity of purified p85α/p110α and p85β/p110α by using distinct phosphoinositides. p85α/p110α showed higher kinase activity for PtdIns substrate; in contrast, p85β/p110α phosphorylated PtdIns(4,5)P_2 more efficiently than p85α/p110α (Fig. S8*A*). We also tested HA-p85β/p110α and HA-p85α/p110α activity in HA immune complexes by using a mixture of PtdIns, PtdIns(4)P, and PtdIns(4,5)P_2 (Fig. 4*C*), which confirmed p85β/p110α preference for the physiological substrate PtdIns(4,5)P_2. PtdIns(3)P is a lipid product generated only in in vitro reactions using purified p110, but does not markedly increase in cells after p110 activation, when the products generated are PtdIns(3,4,5)P_3 and PtdIns(3,4)P_2 (21). Despite this distinct PI3K substrate specificity in vitro and in vivo, the observation that p85β/p110α phosphorylates PtdIns (4,5)P_2 more efficiently than p85α/p110α in the same conditions (Fig. 4*C*) suggests higher intrinsic affinity of p85β/p110α for PtdIns(4,5)P_2.

p85β Controls Tumor Progression in Mouse. p85β expression activates basal PI3K activity and might facilitate cell transformation

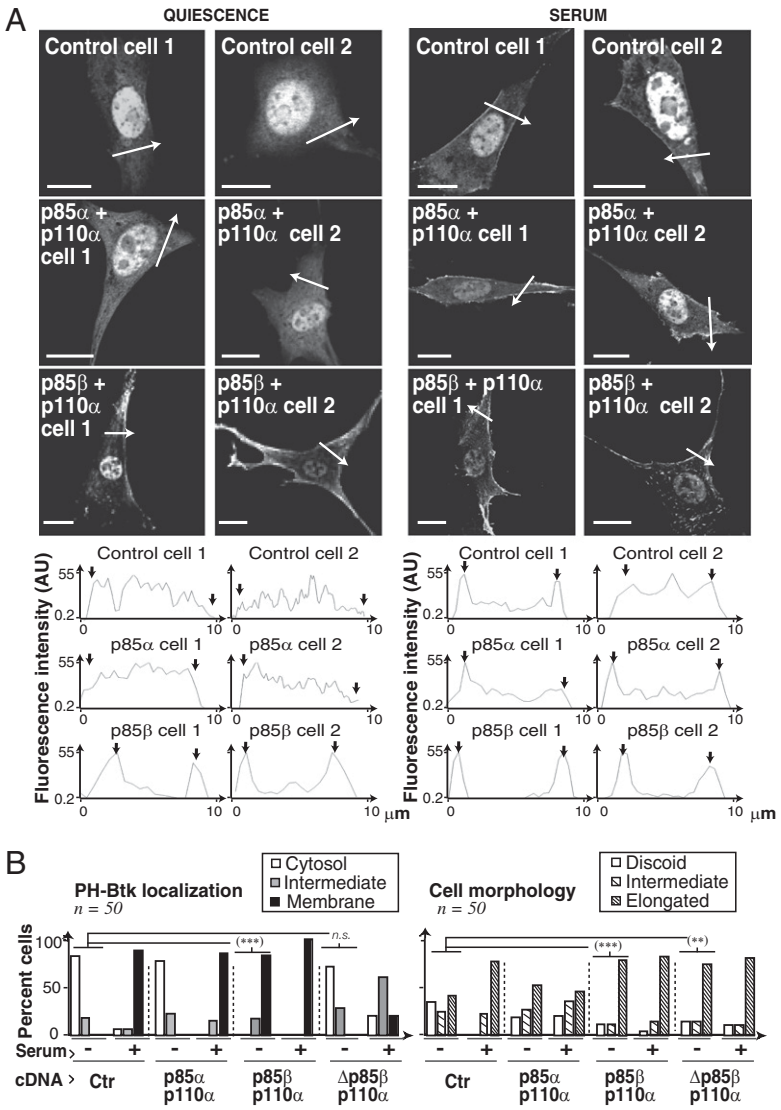

Fig. 3. p85β enhances plasma membrane PIP_3 levels. (*A*) NIH 3T3 cells were cotransfected with GFP-Btk-PH and cDNAs encoding p85α/p110α or p85β/p110α (24 h), then incubated in serum-free medium for 2 h (*Left*); some were activated with serum for 15 min (*Right*). PIP_3 localization (Btk-PH signal) was analyzed by fluorescence microscopy. Graphs show fluorescence intensity [in arbitrary units (AU)] in the sections indicated by white arrows. Arrows in graphs indicate the cell membrane. (*B*) Graphs show the percentage of cells with PIP_3 signal at cell membrane, cytosol, or both, and the percentage of cells with discoid, elongated, or intermediate morphology. (Scale bar: 15 μm.) $^{***}P < 0.001$ and $^{**}P < 0.01$ by χ^2 test.

or invasion. p85β, but not p85α, triggered cell transformation in a focus formation assay and enhanced cell invasion (Fig. 4 *D* and *E*); in agreement, p85β knockdown reduced invasion of NIH 3T3 cells as well as that of BLM and HT1080 cells, both of which are highly invasive (Fig. S8*B*).

To study the influence of p85β deletion on carcinogenesis in a genetically controlled model, we used azoxymethane/dextran sodium sulfate (AOM/DSS) inflammation-dependent mouse colon carcinogenesis. As *Pik3r2* regulates inflammation (7), *Pik3r2*$^{-/-}$ and WT mice were transplanted with WT bone marrow (BM) before AOM/DSS treatment (Fig. 5*A* and Fig. S9*A*). In WT and *Pik3r2*$^{-/-}$ mice, most tumors generated were flat colon carcinomas that did not differ in distribution of tumor size; tumor number was nonetheless significantly lower in p85β-deficient mice (Fig. 5*A*). To determine whether BC responds to decreased p85β levels, we examined eight BC cell lines with higher p85β expression than p85α expression, and half of them responded with reduced proliferation; we selected two representative lines for careful examination (Fig. S9*B*). MDA-MB231 cells grew more rapidly and were unaffected by a reduction in p85β or p85α levels; in contrast, p85β siRNA-transfected MDA-MB468 cells showed reduced growth and underwent cell death (Fig. S9*B*). As well as acting as a BC invasion marker, p85β thus determines survival of some BC cells; future studies will address the genetic background needed for p85β-dependent BC cell survival.

To test the effect of increased p85β expression on carcinogenesis, we augmented p85β levels by retroviral infection of the BM and analyzed tumor progression in the N-ethyl-N-nitrosourea (ENU) thymic lymphoma model in SCID mice. We infected SCID mouse BM with p85β-encoding retroviruses (Fig. S9*C*). Mice received transplants of control or p85β-infected SCID BM and, after ∼1 mo, were treated with ENU. Tumors appeared at ∼7.5 mo in controls and at ∼3 mo in p85β-expressing mice, reducing their lifespan (Fig. 5*D*). A larger percentage of p85β-expressing mice showed spleen metastases compared with controls, as determined by analysis of tumor phenotype (Fig. 5*E* and Fig. S9*D*). Increased *pik3r2* mRNA expression in mice was confirmed by qPCR (Fig. 5*E*). p85β expression and PKB activation in

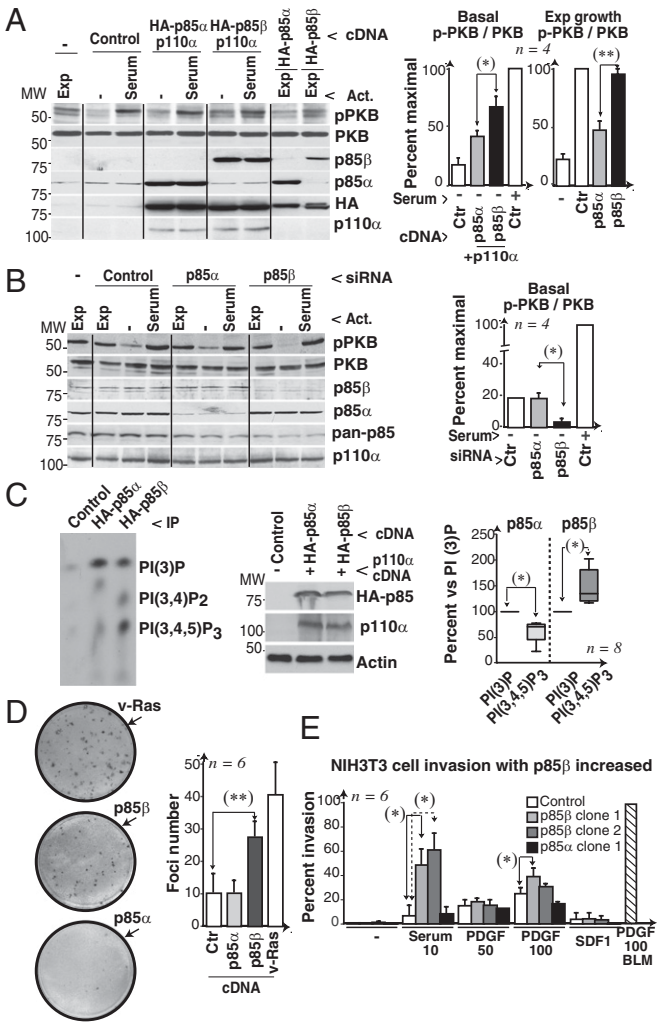

Fig. 4. Enhanced PI3K pathway activation in p85β-expressing cells. (*A*) U2OS cells transfected with HA-p85α or -β alone or in combination with p110α (48 h) were serum-deprived (2 h); some were then serum-stimulated (10%, 10 min), and other samples were maintained in exponential growth (Exp). PI3K and p-PKB levels were tested by WB. Graphs show the percentage of signal in each lane compared with maximum (100%, control cells with serum). (*B*) U2OS cells were transfected with control, p85β, or p85α siRNA (48 h) and tested as in *A*. (*C*) Extracts from COS-7 cells transfected with HA-p85α/p110α or HA-p85β/p110α (48 h) were analyzed by WB or IP with anti-HA Ab and tested in a kinase assay by using a mixture of PtdIns, PtdIns (4)P, and PtdIns (4,5)P2. Graphs show the PtdIns (3,4,5)P_3 signal compared with the PtdIns (3)P signal (100%; mean ± SD, $n = 8$). (*D*) Representative focus formation assay of NIH 3T3 cells transfected with p85α, p85β, or V12-Ras (positive control); the graph shows mean focus number ± SD ($n = 6$ assays). (*E*) Percent matrigel invasion by NIH 3T3 cell lines expressing p85α or p85β compared with maximum (BLM cells with 100 ng/mL PDGF). Invasion assays ($n = 6$) were performed in serum (10% or 20%), PDGF (in ng/mL as indicated) or SDF1 (100 ng/mL). *$P < 0.05$ and **$P < 0.01$ by Student *t* test.

lymphomas was confirmed by WB (Fig. S9*E*); lymphomas were otherwise similar in both mouse types (Fig. 5*F*). Increased p85β expression thus regulates tumor progression in mammals.

Discussion

We showed that increased p85β expression correlates with PI3K pathway activation and tumor progression in BC and CC. Accordingly, modulation of p85β levels regulated tumor progression in mouse. p85β expression augmented plasma membrane PIP_3 levels and activation of the PI3K effector PKB in the absence of stimulus, and triggered focus formation and cell invasion, suggesting that p85β regulates tumor progression.

p110α associates at a 1:1 ratio with p85α or p85β (6). Similar to p85α, p85β mediates p110 translocation to receptors at the cell membrane; indeed, double *pik3r1*/*pik3r2*-deficient mice die earlier than those with single deletions (7, 8, 22). Both p85α/p110α- and p85β/p110α-expressing cells showed maximal PI3K activation only after stimulation, suggesting that both p85 subunits restrict p110α activation, possibly in a distinct manner. Nonetheless, in the absence of stimulus, p85β alone and p85β/p110α induced moderate PI3K activation. The higher affinity of p85β than of p85α for membrane PtdIns(4,5)P_2 might result in spontaneous p85β translocation to the cell membrane and partial p110α or β activation. Whereas the effects of p85β on PI3K pathway activation were p110-dependent, morphological effects were at least partially kinase-independent.

With the exception of the brain, most normal tissues express higher levels of p85α than of p85β (refs. 5–7 and data from ref. 23). It is thus possible that in physiological conditions, p85β expression increases only when higher basal PI3K activity is needed. Whereas p85α-deficient mice die perinatally, p85β-deficient mice grow normally and show only moderate immunological defects (7, 8). Somatic mutations in *PIK3R1* are more frequent than those in *PIK3R2*; p85α mutations concentrate in critical hotspots and activate p110 (9, 10, 24). In contrast, the few mutations described in p85β do not concentrate at hotspots and show a modest functional difference with WT p85β (24). Moreover, whereas genetic deletion of p85β impaired tumorigenesis (Fig. 5), p85α deletion increases this process (11). This is concordant with the observation that *PIK3R1* expression is often reduced, whereas *PIK3R2* expression is increased, in BC and CC. Although the tumor sample analyzed here is small, the tendency toward increased *PIK3R2* expression in BC and CC is supported by other gene expression studies (data from ref. 25). p85β expression might have distinct effects in different tumor types. p85β deletion in heterozygous *Pten*$^{+/-}$ mice does not change the incidence of intestinal polyps (26); the different tumor type, stage, or *Pten* status might explain the absence of an effect. Several studies indicate that p85 associates with and regulates PTEN. p85β might also affect tumor progression through distinct binding or action on PTEN, although both p85α and p85β associate with PTEN (27).

We show here that p85β levels are frequently increased in CC and BC, an increase that correlated with PI3K pathway activation and tumor progression. We confirmed that p85β levels regulate tumor progression in vivo, that the p85β/p110α complex shows preference for the physiological substrate PtdIns(4,5)P_2, and that p85β expression induces cell transformation and invasion. The contribution of p85β to tumor progression indicates new therapeutic possibilities for cancer treatment through interference with p85β action (e.g., phospholipid analogues or siRNA). Analysis of p85β levels could complement diagnosis and help to identify which patients would benefit from classical or PI3K-targeted chemotherapy.

Materials and Methods

cDNAs. p85β was subcloned into pSG5, and an HA epitope was added in-frame at the N terminus. The p85β ATG codon was replaced with a CCG codon (proline) and the HA-tag ATG codon was maintained (Quik-Change mutagenesis kit; Stratagene). siRNA for human p85β and control were from Invitrogen; siRNA for human p85α was from Dharmacon; and shRNA for mouse p85β was from OriGene.

Human Tumor Analysis, WB, and PI3K Assays. BC and CC and adjacent normal tissue samples were provided by the Tissue Bank Network funded by the Molecular Pathology Program of the Spanish National Cancer Center. CCs were classified according to modified Dukes criteria (D0 to DC). BCs were graded using the Bloom–Richardson criteria (grades 1–3), and classified as luminal A, B, HER2$^+$, or basal-type (14–16). p85 protein content was

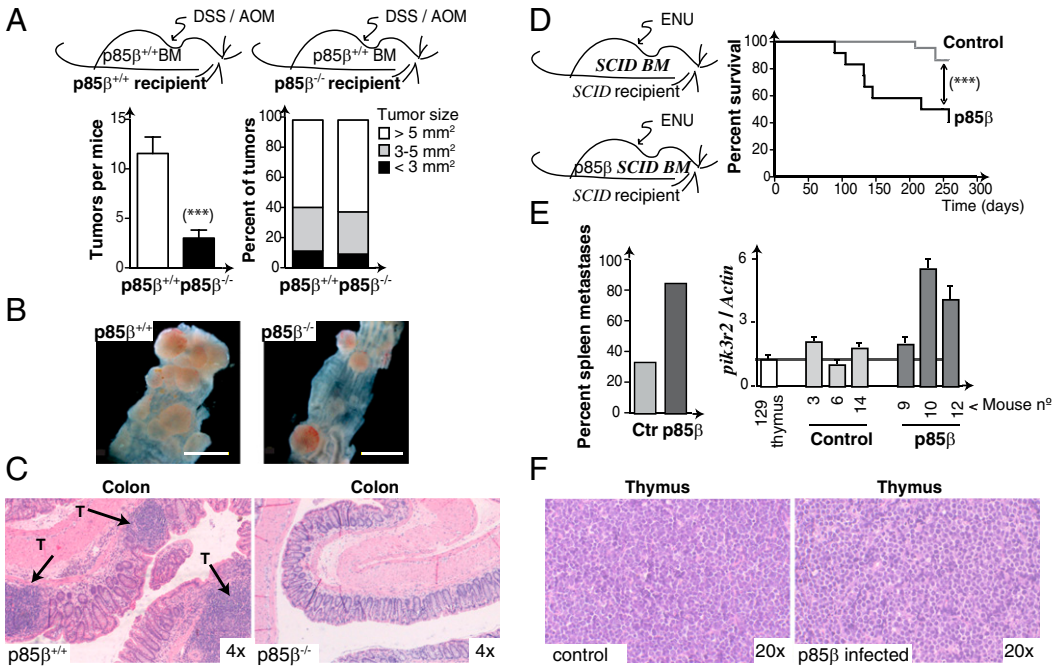

Fig. 5. p85β controls tumor progression in vivo. (*A*) Colon carcinogenesis was induced by AOM/DSS treatment of $p85\beta^{+/+}$ and $p85\beta^{-/-}$ mice 1 mo after transplantation with WT ($p85\beta^{+/+}$) BM. Tumor multiplicity and size in $p85\beta^{+/+}$ and $p85\beta^{-/-}$ mice after AOM/DSS treatment (mean ± SD, n = 12; $***P < 0.001$ by Student *t* test). (*B*) Representative images from $p85\beta^{+/+}$ and $p85\beta^{-/-}$ mice showing tumors in the distal colon. (Scale bar: 5 mm.) (*C*) H&E-stained colon sections show tumors in AOM/DSS-treated $p85\beta^{+/+}$ and $p85\beta^{-/-}$ mice. Arrows indicate tumor masses (T). (*D*) Lymphomagenesis was induced in SCID mice after transplantation with control or p85β-infected BM, followed by ENU treatment (*Left*). Kaplan–Meier survival curves (*Right*); $***P < 0.001$ by Mantel–Cox test (n = 15 p85β, n = 22 controls). (*E*) Percentage of mice with spleen metastases of the thymic lymphoma (*Left*). qPCR shows pikr2 expression in control and p85β-transduced SCID mice tumors (*Right*). (*F*) Thymic lymphomas from control or p85β-transduced SCID mouse. Original magnification indicated.

examined by WB and mRNA levels examined by qPCR. WB and PI3K assays were performed as described earlier (7). Additional methods are detailed in *SI Materials and Methods*.

ACKNOWLEDGMENTS. We thank D. Fruman for donation of p85β-deficient mice; A. Klippel for anti-p110α Ab; T. Balla for the GFP-PH-Btk plasmid; J. W. G. Janssen for pT7/T3-U19-p85β; M. Morente and L. Cereceda for support at the Centro Nacional de Investigaciones Oncológicas tumor bank; J. Teixido, L. Sanz, L. Barrios, P. Cuesta, M. Muñoz, A. Zaballos, L. Almonacid, M. Llorente, and M. García-Gallo for technical help; and R. Hartong and C. Mark for editorial assistance. This work was supported by a Formation of University Professors Predoctoral Fellowship (to I.C.); grants from the Spanish Association Against Cancer; Spanish Ministry of Science and Innovation Consolider OncoBIO Grants SAF2007-63624, SAF2007-60490, and SAF2010-21019; Network of Cooperative Research in Cancer Grant RD07/0020/2020; Madrid Regional Government Grant S-BIO-0189/06; and the Sandra Ibarra Foundation.

1. García Z, Kumar A, Marques M, Cortes I, Carrera AC (2006) PI3K controls early and late events in mammalian cell division. *EMBO J* 25:655–661.
2. Marone R, Cmiljanovic V, Giese B, Wymann MP (2008) Targeting PI3K: Moving towards therapy. *Biochim Biophys Acta* 1784:159–185.
3. Kok K, Geering B, Vanhaesebroeck B (2009) Regulation of PI3K expression in health and disease. *Trends Biochem Sci* 34:115–127.
4. Fruman DA, Cantley LC, Carpenter CL (1996) Structural organization and alternative splicing of the murine PI3K p85 alpha gene. *Genomics* 37:113–121.
5. Ueki K, et al. (2002) Molecular balance between the regulatory and catalytic subunits of PI3K regulates cell signaling and survival. *Mol Cell Biol* 22:965–977.
6. Geering B, Cutillas PR, Nock G, Gharbi SI, Vanhaesebroeck B (2007) Class IA PI3K are obligate p85-p110 heterodimers. *Proc Natl Acad Sci USA* 104:7809–7814.
7. Alcazar I, et al. (2009) p85beta PI3K regulates CD28 coreceptor function. *Blood* 113: 3198–3208.
8. Fruman DA, et al. (1999) Impaired B cell development and proliferation in absence of PI3K p85alpha. *Science* 283:393–397.
9. Yu J, et al. (1998) Regulation of the p85/p110 PI3K: stabilization and inhibition of the p110alpha catalytic subunit by the p85 regulatory subunit. *Mol Cell Biol* 18:1379–1387.
10. Philp AJ, et al. (2001) The PI3K p85alpha gene is an oncogene in human ovarian and colon tumors. *Cancer Res* 61:7426–7429.
11. Vogt PK, Kang S, Elsliger MA, Gymnopoulos M (2007) Cancer-specific mutations in PI3K. *Trends Biochem Sci* 32:342–349.
12. Liu P, Cheng H, Roberts TM, Zhao JJ (2009) Targeting the PI3K pathway in cancer. *Nat Rev Drug Discov* 8:627–644.
13. Guertin DA, Sabatini DM (2007) Defining the role of mTOR in cancer. *Cancer Cell* 12: 9–22.
14. DeVita VT, Hellman S, Rosenberg SA, eds (2005) *Cancer: Principles and Practice of Oncology* (Lippincott Williams and Wilkins, Philadelphia).
15. Bloom HJ, Richardson WW, Harries EJ (1962) Natural history of untreated breast cancer (1805-1933). Comparison of untreated and treated cases according to histological grade of malignancy. *BMJ* 2:213–221.
16. Sørlie T, et al. (2001) Gene expression patterns of breast carcinomas distinguish tumor subclasses with clinical implications. *Proc Natl Acad Sci USA* 98:10869–10874.
17. Guo C, et al. (2008) The noncoding RNA, miR-126, suppresses the growth of neoplastic cells by targeting PI3K signaling and is frequently lost in colon cancers. *Genes Chromosomes Cancer* 47:939–946.
18. Lujambio A, et al. (2008) A microRNA DNA methylation signature for human cancer metastasis. *Proc Natl Acad Sci USA* 105:13556–13561.
19. Saito K, Scharenberg AM, Kinet JP (2001) Interaction between the Btk PH domain and phosphatidylinositol-3,4,5-trisphosphate directly regulates Btk. *J Biol Chem* 276: 16201–16206.
20. Myers MP, et al. (1998) The lipid phosphatase activity of PTEN is critical for its tumor supressor function. *Proc Natl Acad Sci USA* 95:13513–13518.
21. Auger KR, Serunian LA, Soltoff SP, Libby P, Cantley LC (1989) PDGF-dependent tyrosine phosphorylation stimulates production of novel polyphosphoinositides in intact cells. *Cell* 57:167–175.
22. Brachmann SM, et al. (2005) Role of PI3K regulatory isoforms in development and actin rearrangement. *Mol Cell Biol* 25:2593–2606.
23. Genevestigator (2012) GENEVESTIGATOR Biomedical. Available at www.genevestigator.com. Accessed February 25, 2012.
24. Cheung LW, et al. (2011) High frequency of PIK3R1 and PIK3R2 mutations in endometrial cancer elucidates a novel mechanism for regulation of PTEN protein stability. *Cancer Discov* 1:170–185.
25. Oncomine (2012) Oncomine 4.4 Research Edition. Available at www.oncomine.org. Accessed May 25, 2012.
26. Luo J, et al. (2005) Modulation of epithelial neoplasia and lymphoid hyperplasia in PTEN+/– mice by the p85 regulatory subunits of PI3K. *Proc Natl Acad Sci USA* 102: 10238–10243.
27. Rabinovsky R, et al. (2009) p85 Associates with unphosphorylated PTEN and the PTEN-associated complex. *Mol Cell Biol* 29:5377–5388.